

Open Fermi-Hubbard model: Landauer's *vs.* master equation approaches

Andrey R. Kolovsky^{1,2}

¹*Kirensky Institute of Physics, 660036 Krasnoyarsk, Russia and*

²*Siberian Federal University, 660041 Krasnoyarsk, Russia*

(Dated: November 18, 2020)

We introduce a simple model for the quantum transport of Fermi particles between two contacts connected by a lead. It generalizes the Landauer formalism by explicitly taking into account the relaxation processes in the contacts. We calculate the contact resistance and non-equilibrium quasi-momentum distribution of the carriers in the lead and show that they strongly depend on the rate of relaxation processes.

I. INTRODUCTION

Recently much attention has been paid to dynamics and non-equilibrium states of open many-body systems [1–16]. Here the term ‘open’ means that the system of interest is coupled to a bath and, hence, generally neither the system energy nor the number of particles in the system are conserved. Typical examples of open many-body systems are the open Fermi-Hubbard and Bose-Hubbard models [3, 5, 8, 10, 13, 14, 16] which are supposed to describe the current of fermionic or bosonic particles between two reservoirs (the contacts) connected by a one-dimensional lattice (the lead). The mathematical framework of the models is the master equation for the reduced density matrix of the carriers in the lattice with two relaxation terms acting on the first and the last sites of the lattice. Remarkably, these models can be tackled analytically or semi-analytically, leading to a number of important conclusions. In particular, it was shown in the recent work [16] that in the case of Bose particles the inter-particle interactions result in a change of the ballistic transport regime, where the current across the lattice is independent of the lattice length L , to the diffusive transport, where the current is inverse proportional to L .

Although the open Fermi- and Bose-Hubbard models are important in the field of quantum transport, they have a limited applicability because they rely on the Markovian master equation which is only justified for high-temperature reservoirs [11, 14, 17]. The case of low-temperature particle reservoirs, which is of particular interest in solid-state physics, remains a challenge. A popular approach to a non-Markovian bath is the stochastic Schrödinger equation with the correlated noise [18–21]. As shown in Ref. [21], this leads to an infinite set of the coupled Lindblad-like master equations which should be truncated to a finite set to ensure a given accuracy. Unfortunately, the application of this method to the open Hubbard chains looks unfeasible for the moment. In the present work we explore a different approach which allows us to stay within the Markovian approximation in spite of the fact that the reduced density matrix of the carriers in the chain does not obey a Markovian master equation. The idea is to use the hierarchical reservoirs where the contacts are both part of the system and the

larger reservoirs.

The structure of the paper is the following. In the next section we introduce a simple model where the Hubbard chain is dressed by the contacts. In Sec. III we analyze the current of the Fermi particle across the chain as the function of the model parameters and calculate non-equilibrium distributions of the carriers over the Bloch states for the carriers in the contacts and the lead. The relation to the Landauer equation is discussed in Sec. IV. Finally, the concluding Sec. V summarizes the obtained results and indicates some prospects of the further research.

II. MODEL

Let us consider two contacts connected by the Hubbard chain (see Fig. 1),

$$\hat{H} = \hat{H}_L + \hat{H}_R + \hat{H}_s + \hat{H}_\epsilon^{(L)} + \hat{H}_\epsilon^{(R)}. \quad (1)$$

In Eq. (1) \hat{H}_L and \hat{H}_R are Hamiltonians of the left and right contacts, \hat{H}_s is the Hamiltonian of the carriers in the chain, and $\hat{H}_\epsilon^{(j)}$, where $j = L, R$, are the coupling Hamiltonians.

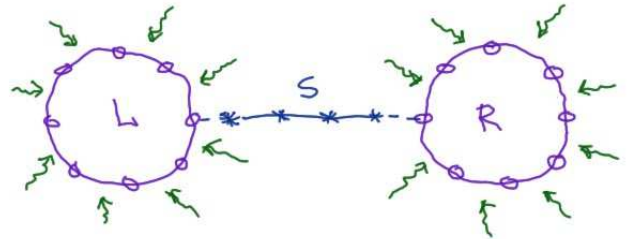


FIG. 1: Schematic presentation of the model. Wavy arrows indicate the particle exchange between the contacts and reservoirs.

The Hamiltonians of the contacts read

$$\hat{H}_j = \sum_k E_k \hat{b}_k^\dagger \hat{b}_k, \quad E_k = -J \cos\left(\frac{2\pi k}{M}\right), \quad (2)$$

where \hat{b}_k^\dagger and \hat{b}_k are the creation and annihilation operators which create or annihilate a particle in the Bloch state with the quasimomentum $\kappa = k/M$. Notice that these operators, as well as the Hamiltonian parameters, also carry the index j which we omit here not to overburden the equation. The contacts are assumed to be a part of the larger particle reservoirs which enforce the relaxation of the reduced density matrices $\hat{R}^{(j)}(t)$ of the isolated contacts into the equilibrium state given by the Fermi-Dirac distribution for the fermionic carriers and Bose-Einstein distribution for the bosonic carriers,

$$n_k = \text{Tr}[\hat{b}_k^\dagger \hat{b}_k \hat{R}(t = \infty)] = \frac{1}{e^{\beta(E_k - \mu)} \mp 1}. \quad (3)$$

To be certain, from now on we shall consider the spinless fermions and zero reservoir temperature. Then the explicit form of the Lindblad relaxation operator is

$$\mathcal{L}(\hat{R}) = -\frac{\gamma}{2} \sum_{|k| < k_F} \left(\hat{b}_k \hat{b}_k^\dagger \hat{R} - \hat{b}_k^\dagger \hat{R} \hat{b}_k + \hat{R} \hat{b}_k^\dagger \hat{b}_k \right), \quad (4)$$

if $|k| < k_F$ and

$$\mathcal{L}(\hat{R}) = -\frac{\gamma}{2} \sum_{|k| > k_F} \left(\hat{b}_k^\dagger \hat{b}_k \hat{R} - \hat{b}_k \hat{R} \hat{b}_k^\dagger + \hat{R} \hat{b}_k \hat{b}_k^\dagger \right), \quad (5)$$

if $|k| > k_F$, where k_F is determined by the Fermi energy of the corresponding reservoir through the relation $E_F = -J \cos(2\pi k_F/M)$ and γ is the relaxation constant.

For fermions in the chain we elect to work in the Wannier basis. Then the chain Hamiltonian is given by the tight-binding model for the spinless fermions,

$$\hat{H}_s = -\frac{J}{2} \left(\sum_{l=1}^{L-1} \hat{c}_{l+1}^\dagger \hat{c}_l + h.c. \right), \quad (6)$$

where operator \hat{c}_l^\dagger (\hat{c}_l) creates (annihilates) a fermion in the l -th site of the chain. To simplify the analysis we assume that the hopping constant J in Eq. (6) coincides with that in Eq. (2). This allows us to use J as the energy measurement unit.

Finally, the coupling operator between the left contact and the chain is

$$\hat{H}_\epsilon^{(L)} = \frac{\epsilon}{\sqrt{M}} \left(\hat{c}_1^\dagger \sum_{k=1}^M \hat{b}_k e^{i\frac{2\pi m}{M}k} + h.c. \right), \quad (7)$$

and the coupling operator between the chain and the right contact has similar form where the operator \hat{c}_1^\dagger is substituted by the operator \hat{c}_L^\dagger .

The evolution of the system (1) is assumed to obey the Markovian master equation

$$\frac{d\hat{R}}{dt} = -i[\hat{H}, \hat{R}] + \mathcal{L}_L(\hat{R}) + \mathcal{L}_R(\hat{R}), \quad (8)$$

where $\hat{R} = \hat{R}(t)$ now denotes the total density matrix of the composed system ‘contacts+chain’. In the considered case of the spinless fermions the size of this matrix is obviously given by the equation,

$$\mathcal{N} = \sum_{n=0}^N \frac{N!}{n!(N-n)!} = 2^N, \quad (9)$$

where the parameter N is the total number of the single-particle states, $N = M_L + L + M_R$. The density matrix \hat{R} carries full information about the system which we actually do not need for our purposes. Indeed, to predict the current between the contacts it suffices to know the single particle density matrix (SPDM) of the size $N \times N$ which is defined according to the equation

$$\rho_{k,l}^{(i,j)}(t) = \text{Tr}[\hat{d}_k^{(i)} \hat{d}_l^{(j)} R(t)]. \quad (10)$$

(Here we use the common notation for the creation and annihilation operators appearing in the problem, where the superindexes i and j now take one of the three meaning – L for the left contact, s for the chain, and R for the right contact.) Our particular interest is the block $\rho_{l,m}^{(s,s)}$ which is the SPDM of the carriers in the chain. Knowing this block one finds the current as

$$j(t) = \text{Tr}[\hat{j} \hat{\rho}^{(s,s)}(t)], \quad (11)$$

where \hat{j} is the current operator, $j_{l,m} = J(\delta_{l,m+1} - \delta_{l+1,m})/2i$. Alternatively, one finds the current by using the equation

$$j(t) = 2 \sum_{k>0} J \sin\left(\frac{2\pi k}{M}\right) f(k, t), \quad (12)$$

$$f(k, t) = \tilde{\rho}_{k,k}^{(s,s)}(t) - \tilde{\rho}_{-k,-k}^{(s,s)}(t), \quad (13)$$

where $\tilde{\rho}^{(s,s)}$ is the matrix $\hat{\rho}^{(s,s)}$ in the momentum representation, i.e., the Fourier transform of $\hat{\rho}^{(s,s)}$.

Next we use the fact that the master equation (8) has a quadratic form with respect to creation and annihilation operators. In this case one can obtain a closed set of equations for the SPDM elements. Substituting Eq. (10) into Eq. (8) we get

$$\frac{d\rho_{k,l}^{(i,j)}}{dt} = -i[\hat{H}, \rho]_{k,l}^{(i,j)} - \gamma B^{(i,j)} \rho_{k,l}^{(i,j)} + \gamma A_{k,l}^{(i,j)}, \quad (14)$$

where $B^{(L,L)} = B^{(R,R)} = B^{(L,R)} = B^{(R,L)} = 1$, $B^{(s,s)} = 0$, $B^{(s,L)} = B^{(L,s)} = B^{(s,R)} = B^{(R,s)} = 0.5$, and $A_{k,l}^{(i,j)} = 0$ except the elements $A_{k,k}^{(j,j)}$ which are equal to unity for $|k| < k_F^{(j)}$ of the respective contact. It is easy to see from Eq. (14) that for vanishing coupling constant ϵ the density matrices of the contacts relax to the diagonal matrices with the diagonal elements obeying the Fermi-Dirac distribution (3). However, if $\epsilon \neq 0$ and $k_F^{(R)} \neq k_F^{(L)}$ the system relaxes to a non-equilibrium state with the stationary current \bar{j} flowing between the contacts. In what follows we analyze this non-equilibrium state in more detail.

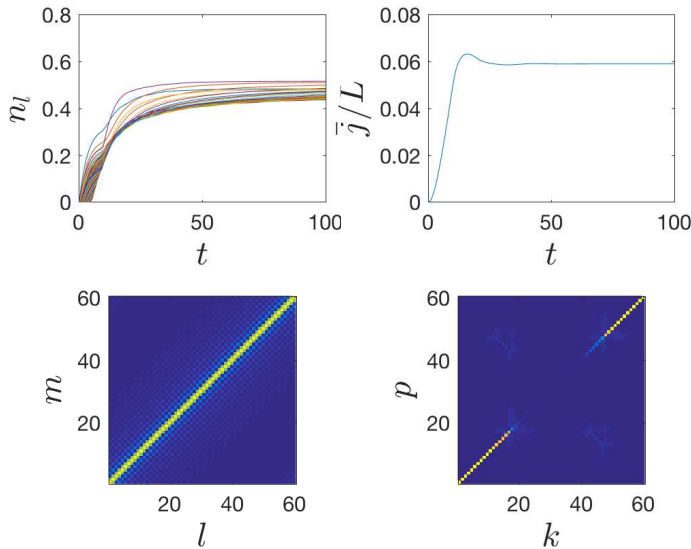


FIG. 2: Upper row: Populations of the chain sites (left) and the mean current normalized to the chain length (right) as the functions of time which is measured in the units of the tunneling period. Lower row: Single-particle density matrix of the carriers in the chain at $t = 10^4$ in the coordinate (left) and momentum (right) representation. Parameters are $M_L = M_R = L = 60$, $J = 1$, $\epsilon = 0.5$, $E_F^{(L)} = 0.3$, $E_F^{(R)} = -0.3$, and $\gamma = 0.05$. Initial condition corresponds to the empty system.

III. NUMERICAL RESULTS

We solve Eq. (14) numerically for different system size and different parameter values. The panels (a) and (b) in Fig. 2 illustrate relaxation of the system to the steady state for $M_L = M_R = L = 60$, $J = 1$, $\epsilon = 0.5$, $E_F^{(L)} = 0.3$, $E_F^{(R)} = -0.3$, and $\gamma = 0.05$. The panel (a) shows population dynamics of the lattice sites in the situation where initially there were no particles in the system. It is seen that the site occupations $n_l(t)$ slowly approach the value 0.5. Unlike this slow process, the mean current $j(t)$ rapidly reaches the stationary value $\bar{j}/L \approx 0.06$. Thus, there are two characteristic relaxation times in the system, τ_1 and $\tau_2 \gg \tau_1$, which scale differently with the chain length L . The system reaches its true steady state for $t > \tau_2$, which for the chosen L and the initial condition is about 10^4 tunneling periods.

Next we discuss the stationary SPDM of the carriers in the chain. The lower panels in Fig. 2 show the matrix $\hat{\rho}^{(s,s)}(t = 10^4)$ in the coordinate and momentum representations, respectively. It is seen that the stationary SPDM is approximately diagonal in the momentum representation, where we plot the values of the diagonal elements in Fig. 3 by asterisks connected by the solid line. Additionally, the dash-dotted and dashed lines in Fig. 3 show occupation numbers of the contact Bloch states. It is seen that the Fermi-Dirac distributions of the isolated contacts are slightly perturbed by the lead. On

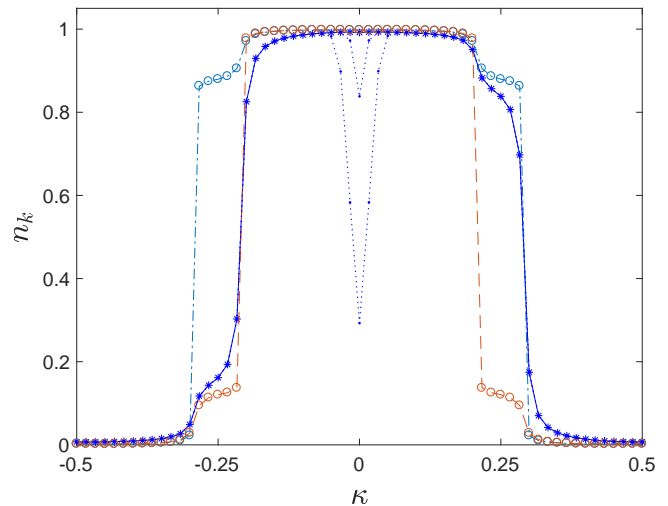


FIG. 3: Stationary momentum distributions (i.e., occupation numbers of the Bloch states) for the carriers in the left contact, dash-dotted line, in the right contact, dashed line, and in the chain, solid line. Additional dotted lines show the momentum distribution of the carriers in the chain at $t = 250$ and $t = 2500$.

the contrary, the momentum distribution of the carriers in the chain strongly deviates from the equilibrium Fermi-Dirac distribution. Namely, it is asymmetric with respect to the reflection $\kappa \rightarrow -\kappa$. Due to this asymmetry we have non-zero net current which can be calculated by using Eqs. (12-13). It is also an appropriate place here to comment on the relaxation time τ_2 . The transient system dynamics for $\tau_1 < t < \tau_2$ is reflected in the momentum distribution as a deep at $\kappa = 0$ (see dotted lines in Fig. 3) which disappears only for $t > \tau_2$. However, since this deep is symmetric with respect to the reflection, it affects neither the function $f(\kappa)$ nor the value of the current as soon as $t > \tau_1$.

Finally we analyze the stationary current as the function the system parameters. To be certain we shall assume $E_F^{(R)} = \Delta E_F/2$, and $E_F^{(L)} = -\Delta E_F/2$. The dashed line in the main panel in Fig. 4 shows the stationary current as the function of ΔE_F for the system size $M_L = M_R = L = 60$. The observed step-like dependence is due to finite size of the contacts. Indeed, increasing the number of states in the contacts two times we double the number of steps. Thus, in the limit $M_L, M_R \rightarrow \infty$ we get a smooth dependence,

$$\frac{\bar{j}}{L} \approx G(\epsilon, \gamma) \Delta E_F, \quad (15)$$

where the conductance $G = G(\epsilon, \gamma)$, also known as the inverse contact resistance, is some function of the relaxation constant γ and the coupling constant ϵ . The dependence (15) is exemplified in Fig. 5. The left panel in Fig. 5 shows the stationary current as the function of ϵ for three different values of the chemical potential difference ΔE_F , where we set the relaxation constant $\gamma = 0.1$. The

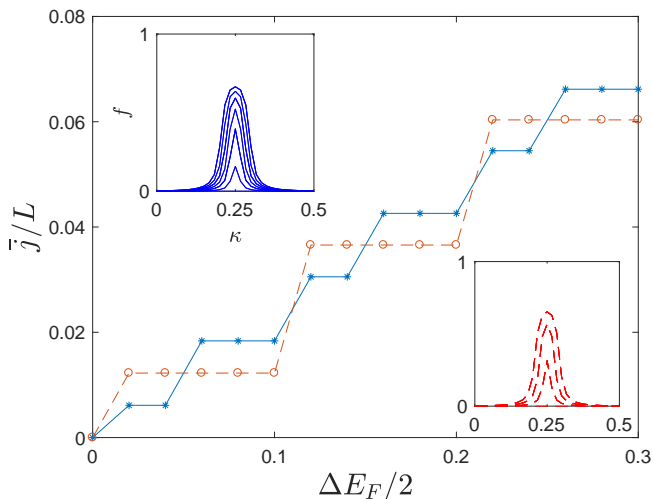


FIG. 4: Stationary current as the function of the chemical potential difference. The chain length is $L = 60$, the contact size are $M_L = M_R = 60$, dashed line, and $M_L = M_R = 120$, solid line. The other parameters are $\epsilon = 0.5$, $E_F^{(R)} = \Delta E_F/2$, $E_F^{(L)} = -\Delta E_F/2$, and $\gamma = 0.125$. The inserts show the function $f(\kappa)$ (only positive part is shown) for every plateau.

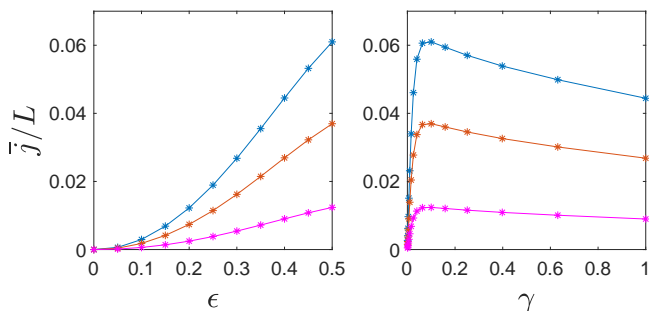


FIG. 5: Left panel: Stationary current as the function of the coupling constant ϵ for $\gamma = 0.1$ and three values of the parameter $\Delta E_F/2 = 0.1, 0.2, 0.3$, from bottom to top. Right panel: Stationary current as the function of the relaxation constant γ for $\epsilon = 0.5$ and three values of the parameter $\Delta E_F/2 = 0.1, 0.2, 0.3$, from bottom to top.

right panel shows the stationary current as the function of γ where we set the coupling constant $\epsilon = 0.5$. Additionally, in Fig. 6 we depict the function $f(\kappa)$ which sheds more light on the observed non-trivial dependence of the current on the relaxation constant γ . This dependence is also discussed in Appendix which contains some analytical results for the stationary SPDM.

IV. IMPERFECT CHAIN

Till now we analyzed the case of the perfect lead. It is interesting to consider an imperfect lead where, according to the Landauer arguments, the stationary current should

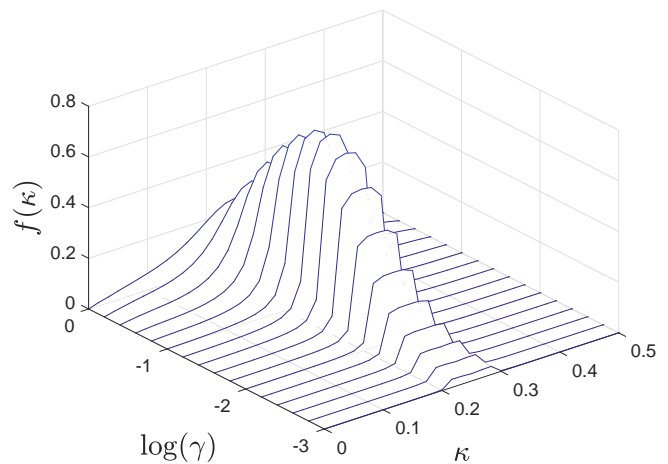


FIG. 6: The function $f(\kappa)$ for the parameters of Fig. 5(b) and $\Delta E_F/2 = 0.3$. Only positive part $\kappa \geq 0$ is shown.

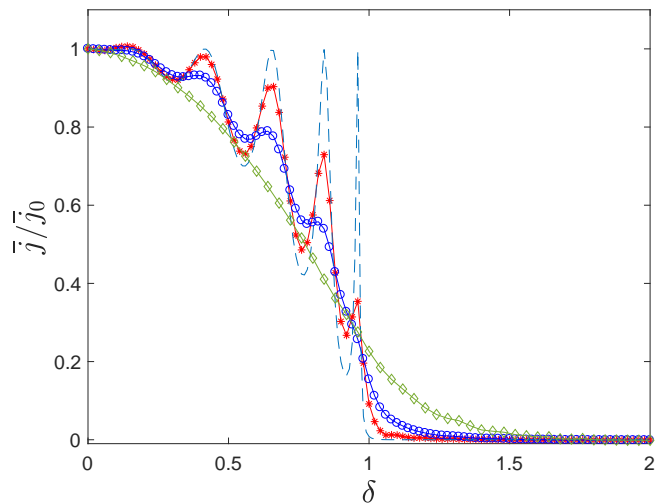


FIG. 7: The stationary current across the chain with the square potential barrier of the 11 sites width and the height δ . Symbols show the ratio \bar{j}/\bar{j}_0 as the function of δ for $\gamma = 0.01$ (asterisks), $\gamma = 0.1$ (circles), and $\gamma = 0.5$ (diamonds). The other system parameters are $\epsilon = 0.5$ and $\Delta E_F/2 = 0.1$. The dashed line is the transmission coefficient of the barrier at $E = E_F = 0$.

obey the equation

$$\bar{j} = \bar{j}_0 |t(E_F)|^2, \quad (16)$$

where $t(E_F)$ is the transmission amplitude for the imperfect chain at the Fermi energy and \bar{j}_0 is the stationary current in the perfect chain. However, Eq. (16) neglects the decoherence effect of reservoirs by approximating the quantum state of the carriers by the plane wave with the quasimomentum k_F . To discuss the validity of Eq. (16) we simulate the system dynamics for the chain with the square potential barrier. The dashed line in Fig. 7 shows the transmission coefficient of the barrier as the function of its height δ . A number of transmission peaks and deeps due to the phenomenon of the resonant above-barrier re-

flexion are clearly seen. The solid lines in Fig. 7 are the ratio \tilde{j}/\tilde{j}_0 for the three different values of the relaxation constant γ . It is seen that the transmission peaks are washed out if γ is increased. Thus, Eq. (16) can be valid only in the limit $\gamma \rightarrow 0$ where, according to the results of Fig. 5(b), the stationary current vanishes.

V. CONCLUSION

We introduced a simple model for the transport of Fermi particles between two contacts with different chemical potentials. The numerical analysis of the model shows that its properties fit well the Landauer approach for the electron transport in the mesoscopic devices [22]. In particular, all relaxation processes in the system take place at the contacts. The main difference with the Landauer approach is that we describe these processes explicitly by using the formalism of the master equation. This allows us to relax the assumption about the ‘re-

flectionless’ contacts and calculate the non-equilibrium distribution of the carriers over the Bloch states for arbitrary value of the relaxation constant γ and the coupling constant ϵ – the parameters which are absent in the standard Landauer theory. Since the constant γ also determines the rate of decoherence in the system, one can address within the framework of the introduced model a number of other questions like, for example, the decoherence effect of reservoirs on the Anderson localization in a disordered chain.

The other prospect of the research is the non-Markovian master equation. For the considered problem one obtains such equation by considering the low-temperature limit and eliminating the contacts. The analysis of this non-Markovian master equation (including various approximations) is of considerable academic interest.

The author acknowledges discussions with D. N. Maksimov and financial support of Russian Science Foundation (RU) through Grant No.19-12-00167.

-
- [1] J. Brantut, J. Meineke, D. Stadler, S. Krinner, and T. Esslinger, *Conduction of ultracold fermions through a mesoscopic channel*, *Science* **337**, 1069 (2012).
 - [2] M. Bruderer and W. Belzig, *Mesoscopic transport of fermions through an engineered optical lattice connecting two reservoirs*, *Phys. Rev. A* **85**, 013623 (2012).
 - [3] A. Ivanov, G. Kordas, A. Komnik, and S. Wimberger, *Bosonic transport through a chain of quantum dots*, *Eur. Phys. J. B* **86**, 345 (2013).
 - [4] C. Nietner, G. Schaller, and T. Brandes, *Transport with ultracold atoms at constant density*, *Phys. Rev. A* **89**, 013605 (2014).
 - [5] T. Prosen, *Exact nonequilibrium steady state of an open Hubbard chain*, *Phys. Rev. Lett.* **112**, 030603 (2014).
 - [6] D. P. Simpson, D. M. Gangardt, I. V. Lerner, and P. Krüger, *One-dimensional transport of bosons between weakly linked reservoirs*, *Phys. Rev. Lett.* **112**, 100601 (2014).
 - [7] R. Labouvie, B. Santra, S. Heun, S. Wimberger, and H. Ott, *Negative differential conductivity in an interacting quantum gas*, *Phys. Rev. Lett.* **115**, 050601 (2015).
 - [8] G. Kordas, D. Witthaut, S. Wimberger, *Non-equilibrium dynamics in dissipative Bose-Hubbard chains*, *Ann. Phys. (Berlin)* **527**, 619 (2015).
 - [9] M. Znidaric, *Relaxation times of dissipative many-body quantum systems*, *Phys. Rev. E* **92**, 042143 (2015).
 - [10] B. Buca and T. Prosen, *Charge and spin current statistics of the open Hubbard model with weak coupling to the environment*, *Phys. Rev. E* **95**, 052141 (2017).
 - [11] A. R. Kolovsky, *Microscopic models of source and sink for atomtronics*, *Phys. Rev. A*, **96**, 011601(R) (2017).
 - [12] M. Lebrat, P. Grisins, D. Husmann, S. Häusler, L. Corman, T. Giamarchi, J.-Ph. Brantut, and T. Esslinger, *Band and correlated insulators of cold fermions in a mesoscopic lattice*, *Phys. Rev. X* **8**, 011053 (2018).
 - [13] A. R. Kolovsky, Z. Denis, and S. Wimberger, *Landauer-Büttiker equation for bosonic carriers*, *Phys. Rev. A* **98** (2018), 043623 (2018).
 - [14] A. R. Kolovsky, and D. N. Maksimov, *Quantum state of the fermionic carriers in a transport channel connecting particle reservoirs*, *Condens. Matter* **2019**, 85 (2019).
 - [15] K. Khani, E. Neri, L. Galantucci, F. Scazza, A. Burchianti, K.-L. Lee, C. F. Barenghi, A. Trombettoni, M. Inguscio, M. Zaccanti, G. Roati, and N. P. Proukakis, *Critical transport and vortex dynamics in a thin atomic Josephson junction*, *Phys. Rev. Lett.* **124**, 045301 (2020).
 - [16] A. A. Bychek, P. S. Muraev, D. N. Maksimov, and A. R. Kolovsky, *Open Bose-Hubbard chain: Pseudoclassical approach*, *Phys. Rev. E* **101**, 012208 (2020).
 - [17] A. R. Kolovsky, *Quantum entanglement and the Born-Markov approximation for an open quantum system*, *Phys. Rev. E* **101**, 062116 (2020).
 - [18] L. Diósi, N. Gisin, and W. T. Strunz, *Non-Markovian quantum state diffusion*, *Phys. Rev. A* **58**, 1699 (1998).
 - [19] Xinyu Zhao, Wufu Shi, Lian-Ao Wu, and Ting Yu, *Fermionic stochastic Schrödinger equation and master equation: An open-system model*, *Phys. Rev. A* **86**, 032116 (2012).
 - [20] Mi Chen and J. Q. You, *Non-Markovian quantum state diffusion for an open quantum system in fermionic environments*, *Phys. Rev. A* **87**, 052108 (2013).
 - [21] D. Suess, W. T. Strunz, and A. Eisfeld, *Hierarchical equations for open system dynamics in fermionic and bosonic environments*, *J. Stat. Phys.* **159**, 1408 (2015).
 - [22] S. Datta, *Electronic Transport in Mesoscopic Systems*, Cambridge University Press, Cambridge, 1995.

VI. APPENDIX

This section contains some analytical results for the stationary SPDM which was analysed numerically in Sec. III. For the sake of completeness we also include results for infinite reservoir temperature.

A. The high-temperature limit

We begin with the case of infinite temperature where the Bloch states of the contacts are equally occupied. The mean occupation numbers \bar{n}_L and \bar{n}_R are obviously determined by the reservoir chemical potentials and, as before, we assume $\mu_L > \mu_R$ that implies $\bar{n}_L > \bar{n}_R$. Assuming additionally $\gamma \gg \epsilon^2$ one justifies the Born-Markov approximation which allows us to obtain the master equation for the reduced density matrix of the carriers in the chain,

$$\frac{d\hat{\rho}}{dt} = -i[\hat{H}_s, \hat{\rho}] + \mathcal{L}_L(\hat{\rho}) + \mathcal{L}_R(\hat{\rho}), \quad (17)$$

where $\hat{\rho}(t) \equiv \hat{\rho}^{(s,s)}(t)$ and the Hamiltonian \hat{H}_s is given in Eq. (6). The explicit form of the Lindblad operator $\mathcal{L}_L(\hat{\rho})$ is

$$\mathcal{L}_L(\hat{\rho}) = -\frac{\tilde{\gamma}}{2} \left[(1 - \bar{n}_L)(\hat{c}_1^\dagger \hat{c}_1 \hat{\rho} - 2\hat{c}_1 \hat{\rho} \hat{c}_1^\dagger + \hat{\rho} \hat{c}_1^\dagger \hat{c}_1) \right. \\ \left. \bar{n}_L(\hat{c}_1 \hat{c}_1^\dagger \hat{\rho} - 2\hat{c}_1^\dagger \hat{\rho} \hat{c}_1 + \hat{\rho} \hat{c}_1 \hat{c}_1^\dagger) \right], \quad (18)$$

where the effective relaxation constant $\tilde{\gamma} \sim \epsilon^2$. The operator $\mathcal{L}_R(\hat{\rho})$ has the similar form with the creation and annihilation operators \hat{c}_1^\dagger and \hat{c}_1 substituted by the operators \hat{c}_L^\dagger and \hat{c}_L . The master equation (17) with the

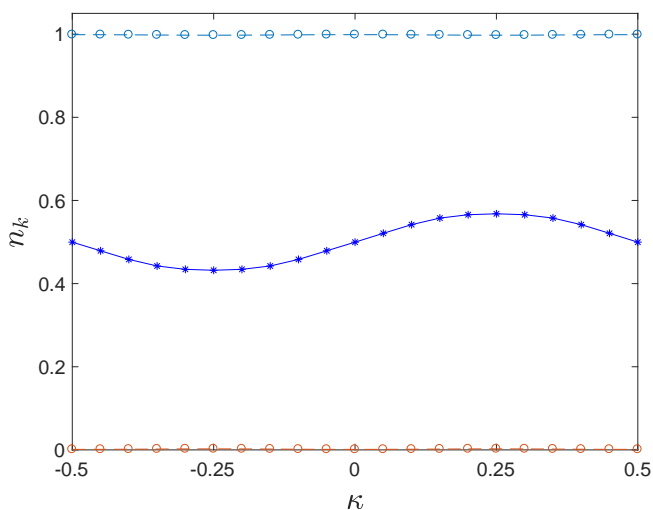


FIG. 8: Stationary momentum distributions for $\beta = 0$. The system parameters are $M_L = M_R = L = 20$, $\bar{n}_L = 1$, $\bar{n}_R = 0$, $\epsilon = 0.2$, and $\gamma = 1.0$.

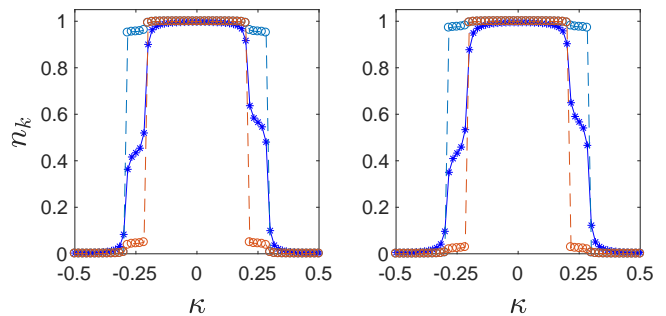


FIG. 9: Stationary momentum distributions calculated according to Eq. (23), left, as compared to the exact result, right. The system parameters are $M_L = M_R = L = 60$, $\Delta E_F = 0.3$, $\epsilon = 0.2$, and $\gamma = 0.05$.

specified relaxation terms can be solved analytically [14] that gives

$$n_k^{(s)} = A + 2B \sin\left(\frac{2\pi k}{L}\right), \quad (19)$$

where

$$A = \frac{\bar{n}_L + \bar{n}_R}{2}, \quad B = \frac{\tilde{\gamma} J}{\tilde{\gamma}^2 + J^2} \frac{\bar{n}_L - \bar{n}_R}{2}. \quad (20)$$

The analytical results (19) is verified in Fig. 8 which shows the occupation numbers $n_k^{(j)}$, $j = L, s, R$, obtained by the straightforward numerical solution of the master equation (14). The sine dependence of $n_k^{(s)}$ on the quasi-momentum is clearly observed. The value of the effective relaxation constant extracted from the depicted numerical data is $\tilde{\gamma} = 0.07$.

B. The low-temperature limit

We come back to the case of zero reservoir temperature. Let us first discuss the limit $\gamma, \epsilon \rightarrow 0$. In this limit the occupation numbers of the Bloch states are

$$n_k^{(L,R)} = \begin{cases} 1, & |k| < k_F^{(L,R)} \\ 0, & |k| > k_F^{(L,R)} \end{cases}, \quad (21)$$

$$n_k^{(s)} = \left(n_k^{(L)} + n_k^{(R)} \right) / 2,$$

and the relaxation terms in the master equation (14) can be approximated by the simpler relaxation term

$$\mathcal{L}(\hat{\rho}) = -\gamma(\hat{\rho} - \hat{\rho}_0), \quad (22)$$

where $\hat{\rho}_0$ is diagonal in the Bloch basis with the elements given by Eq. (21). We mention that this approximation can be justified only for asymptotically large times where $\hat{\rho}(t)$ is close to its stationary value.

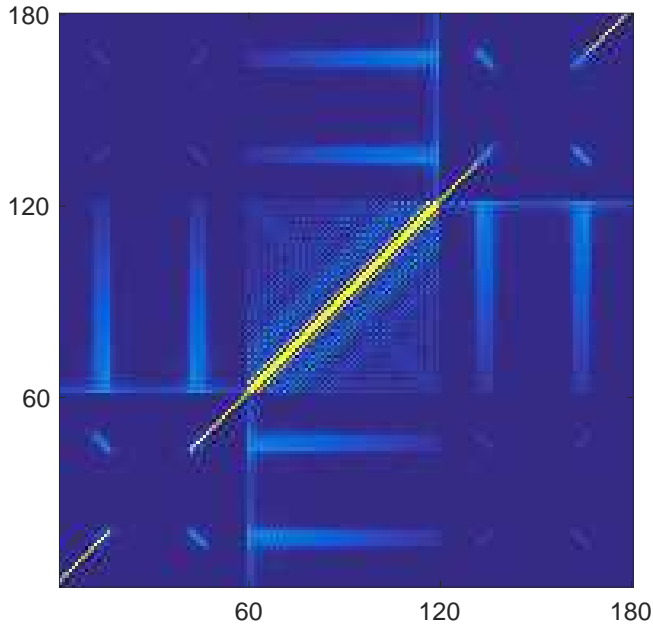


FIG. 10: The stationary SPDM in the original representation. Shown are the absolute values of the matrix elements where the upper limit of the color axis is set to 0.1 to highlight the correlations.

Now we set ϵ to a finite value. Then, using Eq. (22), the stationary solution of the master equation reads

$$\hat{\rho} = \sum_{n,m} \frac{\gamma \langle \psi_n | \hat{\rho}_0 | \psi_m \rangle}{\gamma + i(\mathcal{E}_m - \mathcal{E}_n)} |\psi_n\rangle \langle \psi_m|, \quad (23)$$

where $|\psi_n\rangle$ and \mathcal{E}_n are eigenenergies and eigenstates of the Hamiltonian (1). We found that for $\epsilon \ll J$ Eq. (23) provides a good approximation to the exact stationary SPDM, see Fig. 9.

Concluding this subsection we would like to notice correlations between the chain and the contacts which are absent in the case of infinite reservoir temperature. These correlations are exemplified in Fig. 10 which shows the stationary SPDM in the original basis (i. e., the Wannier basis for the chain and the Bloch basis for the contacts) as a color map. In this figure the central block of the size 60×60 is the reduced density matrix of the carriers in the chain and the left-lower and right-upper blocks are the reduced density matrices of the carriers in the left and right contacts, respectively. Besides ‘contacts-chain’ correlations there also are correlations between $+k$ and $-k$ contact Bloch states for $k_F^{(L)} \leq |k| \leq k_F^{(R)}$.